Preprints of the 19th World Congress
The International Federation of Automatic Control
Cape Town, South Africa. August 24-29, 2014

Feedback stabilization of predator-prey systems for impulsive biological control

Frédéric Grognard *

* *BIOCORE Project-team, INRIA, France (email: frederic.grognard@inria.fr)*

Abstract: In agricultural applications, the introduction of predators is used to control the prey/pests level so that crop damage is limited; however, though a satisfactory equilibrium between predators and prey may exist, it may be unstable. In order to achieve pest control, its stabilization should then be achieved and, since predator releases occur at discrete time instants, we model them through impulses upon which we will build a positive impulsive feedback control law. Our controller is based on the measurement of the state every T time instants followed by the introduction, when necessary, of predators into the system to instantaneously bring their population up to a prescribed level. The proposed controller is shown to lead to the global asymptotic stability of the desired equilibrium for T small; local stability is shown for some larger periods, and some numerical asymptotic analysis is performed.

Keywords: Biological control, impulsive control, predator-prey model, stabilization, global stability, periodic state-dependent resetting

1. INTRODUCTION

Controlling systems in which living organisms play a crucial role is a difficult challenge due to the combination of intrinsic nonlinearities, large uncertainties and positivity of the control. We are particularly interested in the control of predator-prey systems with positive control, in the context of biological control [Hawkins and Cornell, 1999]. The latter is defined as the use of living organisms, the biocontrol agents, to limit or eradicate a pest or pathogen from a crop. These biocontrol agents can take various forms, from parasitoids to bacteria infecting the pest. We will focus on predators feeding on the pests.

In the modeling and analysis of biological control through predator-prey systems, a large effort has been devoted to the periodic introduction of a fixed quantity of predators that is described through impulsive/hybrid models. These aim at pest eradication in some optimal way [Mailleret and Grognard, 2009] and check what bifurcations occur when eradication is not achieved [Liu et al., 2004]. However, pest eradication requires a constant inflow of predators since low levels of prey do not allow predator survival.

We will focus on the stabilization of the system at a prey-level that is non-zero and can sustain a predator population; obviously, this prey level will need to be sufficiently low so as to induce limited harm on the crop, that will be kept implicit in this analysis. We will suppose that the natural positive equilibrium of the uncontrolled system satisfies this constraint. Indeed, predator-prey systems usually have a positive equilibrium where both species are present, but this equilibrium is not necessarily asymptotically stable. Indeed, solutions may tend to a limit cycle as in the Rosenzweig-MacArthur (RMA) model especially if, as desired here, the equilibrium prey-level is low [Rosenzweig, 1971], or the equilibrium can be neutrally stable as in the Lotka-Volterra model [Volterra, 1978]. The non-impulsive feedback stabilization of such equilibria has been rarely tackled and cannot be treated with traditional nonlinear control methods since the control needs to be positive, which is known to render control problems more complex, even in the linear cases [Brammer, 1972]. However, some results can be found in Grognard and Gouzé [2005] for Lotka-Volterra systems and in Grognard et al. [2013] and Meza et al. [2005] for generalized RMA systems.

Combining impulses and feedbacks, we will present a control law for the global asymptotic stabilization of the positive equilibrium of predator-prey systems. We will consider a large family of predator-prey models described with generic trophic functions so as to take some uncertainties into account. The state of the system is measured every T time-instants and predators are then introduced, if necessary, up to some prescribed level. This generates a time-dependent impulsive dynamical system [Haddad et al., 2006] for which we had to develop an ad-hoc stability analysis since the target equilibrium is unstable in the absence of impulses. The proposed controller is in the form of time-dependent resetting controllers as in Bupp et al. [2000] and Haddad et al. [2000].

This paper is structured as follows: the model is presented in Section 2, followed by a description of the control scheme and its global stability analysis in Section 3; what to expect when global stability is not guaranteed is described in Section 4, followed by numerical and asymptotic analyses and some discussions in Section 5.

2. MODELS

We will concentrate on predator-prey models whose positive equilibrium is unstable. The most classical example of such models is the Rosenzweig-Mac Arthur model

(Rosenzweig [1971]) which, in some parametric situations, presents an unstable positive equilibrium. This model writes

$$\begin{cases} \dot{x} = rx\left(1 - \dfrac{x}{K}\right) - \dfrac{bx}{x+h}y \\ \dot{y} = \dfrac{cx}{x+h}y - my \end{cases} \tag{1}$$

with $x \geq 0$ and $y \geq 0$ the prey and predator densities respectively, and with all parameters being positive. The classical exponential growth of the prey of the Lotka-Volterra model has been replaced with logistic growth and the linear predation rate becomes of Holling type II, *eg.* to represent satiation.

In order to set our control problem in a more general context, we propose a generalization of the Rosenzweig-MacArthur model in which we kept the elements that ensure it has the same properties as the classical model:

$$\begin{cases} \dot{x} = f(x) - g(x)y \\ \dot{y} = h(x)y - my \end{cases} \tag{2}$$

with the following hypotheses

Assumption *1.* f, g and h are $\mathcal{C}^1(I\!R^+)$ functions satisfying

(i) $g(0) = 0$, $g'(0) > 0$, and $g(x) > 0$ for $x > 0$;
(ii) $h(0) = 0$, $h(x) > 0$ for $x > 0$, $\exists!$ $x^\star$ such that $h(x^\star) = m$; $h'(x) > 0$ for $x \leq x^\star$;
(iii) $f(0) = 0$, $f'(0) > 0$, and $f(x) > 0$ for $x \in (0, x^\star]$.

These assumptions are quite natural: the hypothesis on the prey growth rate states that prey can grow at small densities; the ones on the predator functional and numerical responses mainly state that predation is unilateral: the prey never preys on the predator.

In that framework, the x nullclines satisfy

$$x = 0 \text{ or } y = \frac{f(x)}{g(x)}$$

and the y nullclines satisfy

$$y = 0 \text{ or } h(x) = m$$

from which, and hypothesis (ii), we deduce that (2) has a positive equilibrium in $I\!R^3_+$: $(x^\star, y^\star)$ with $y^\star = \frac{f(x^\star)}{g(x^\star)} > 0$. Also, it has equilibria of the form $(\bar{x}_i, 0)$ (including the origin) with $\bar{x}_i$ the roots of $f(x)$. These latter equilibria are easily shown to be unstable and the stability of the positive one can be deduced from the Jacobian matrix:

$$\mathcal{J}(x^\star, y^\star) = \begin{pmatrix} \dfrac{f'(x^\star)g(x^\star) - f(x^\star)g'(x^\star)}{g(x^\star)} & -g(x^\star) \\ h'(x^\star)\dfrac{f(x^\star)}{g(x^\star)} & 0 \end{pmatrix}$$

and, when hyperbolic, the equilibrium is locally asymptotically stable if and only if $\det(J) = h'(x^\star)f(x^\star) > 0$ and $\text{trace}(J) = g(x^\star)\left(\frac{f}{g}\right)'(x^\star) < 0$. The former is satisfied thanks to hypothesis (ii) so that this equilibrium is stable if and only if $\left(\frac{f}{g}\right)'(x^\star) < 0$. This means that the stability of this equilibrium is determined by the slope of the x nullcline at equilibrium, as in the classical Rosenzweig-MacArthur model. Since we are considering a stabilization problem, we will concentrate on equilibria that are originally unstable or non hyperbolic (so that the jacobian matrix does not give enough information for their stability analysis):

Assumption *2.* f and g are such that $\left(\frac{f}{g}\right)'(x^\star) \geq 0$

As shown in Saperstone and Yorke [1971], positivity of the control limits the controllability of a system. Since the control cannot steer the system towards all directions in the neighborhood of the equilibrium, there are parts of this neighborhood from which a positive control is inefficient to steer the solution to the equilibrium and no control should be applied. Intuitively, if some eigenvalue of $\mathcal{J}$ is positive real, the solutions would then escape the equilibrium along the eigenvectors, hence the stabilization fails. If the eigenvalues are complex conjugate, the solutions of the uncontrolled system rotate around the equilibrium, so that they will eventually get into a part of the state-space where applying a positive control will be effective for achieving convergence. In order to have the eigenvalues complex, we impose that the discriminant of the characteristic polynomial of $\mathcal{J}$ is negative, giving:

Assumption *3.* Inequality

$$\left[\left(\frac{f}{g}\right)'(x^\star)g(x^\star)\right]^2 < 4h'(x^\star)f(x^\star) \tag{3}$$

is satisfied.

Note that Assumptions 1-3 are satisfied for Lotka-Volterra systems and oftentimes for RMA models when $x^\star$ is small (though (2) indeed generalizes RMA, Ass. 1(ii) or 2 could be violated so that $(x^\star, y^\star)$ could not exist or be stable).

3. MODELLING PREDATORS INTRODUCTION

Setting ourselves in a Biological Control framework, prey x is a pest that damages the (unmodeled) crop, and predator y is the biocontrol agent that will be used to control it. The aim is to devise the introduction strategy of predator y such that the positive equilibrium is asymptotically stable, provided the pest level $x^\star$ does not yield too large damage on the crop.

The introduction scheme is built on the following set-up: every T time instants, which we term measurement instants, the crop is monitored in order to obtain an estimate of both the predator and prey populations. An impulsive control is then applied at that moment by introducing, or not, a certain number of predators. The number of introduced predators will depend on the measured state $(x(nT), y(nT))$: if $y(nT)$ is larger than some predefined $\beta(x(nT))$ determined by the number of prey in the system, no action is taken; otherwise a number of predators is introduced to reach the level $y(nT^+) = \beta(x(nT))$ (where the (nT^+) notation indicates the state of the system right after time nT). The resulting impulsive dynamical system is the following:

$$\begin{cases} \left.\begin{array}{l} \dot{x} = f(x) - g(x)y \\ \dot{y} = h(x)y - my \end{array}\right\} t \neq nT \\ y(nT^+) = \max\left(y(nT), \beta(x(nT))\right) \end{cases} \tag{4}$$

with $n \in I\!N$, and β to be designed. The control effort is non-negative: 0 or $\beta(x(nT)) - y(nT)$.

In order to choose β, we note that the non-trivial x-nullcline, which is $y = \frac{f(x)}{g(x)}$, is positive for all $x \in (0, x^\star]$. Hence, we build β as follows (see Fig. 1)

Assumption *4.* β is a $\mathcal{C}^1$ function that satisfies

- $\beta(x) > 0$ and $\beta'(x) > 0 \; \forall \, x > 0$
- $\beta(x) \leq \frac{f(x)}{g(x)} \; \forall \, 0 \leq x < x^\star$
- $\beta(x) \geq \frac{f(x)}{g(x)} \; \forall \, x > x^\star$

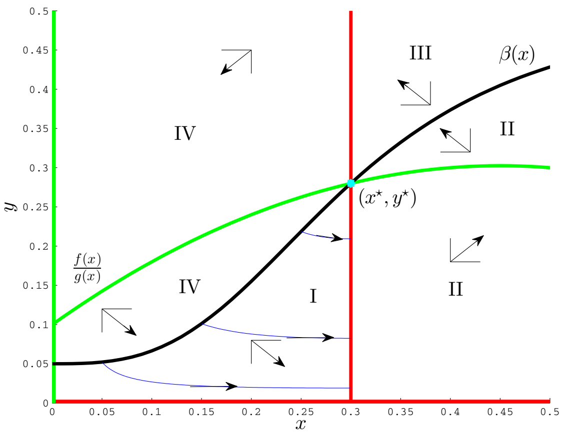

Fig. 1. A β function satisfying Assumption 4 (in black), the x nullcilnes (in green), the y-nullclines (in red), and three solutions (in blue) used to define $\tau(x)$ and $T^\star$. The directions of the field are illustrated and the roman numbers indicate the regions used in the proof of Theorem 1.

Our proof of global asymptotic stability will impose that any solution eventually reaches the manifold $y = \beta(x)$ with $x < x^\star$ and that it roughly slides along it afterwards: once there at time nT^+, it should be back in that zone of the manifold at time $(n+1)T^+$ with $x((n+1)T^+) > x(nT^+)$. The latter can be obtained by ensuring that, for any initial condition $x(nT^+) < x^\star$ with $y(nT^+) = \beta(x(nT^+))$, $x(nT^+) < x(t) < x^\star$ for all $t \in (nT^+, (n+1)T]$. The left inequality is trivial since $\dot{x} > 0$ there and we will show the right inequality to be achievable for T small enough. For that, we first define for all $0 < x_0 < x^\star$ the time $\tau(x_0)$, which is the smallest time it takes for a solution initiated in $(x_0, \beta(x_0))$ to reach the vertical line $x = x^\star$. Function $\tau(x_0)$ is well defined since $\dot{x} > 0$ and $\dot{y} \leq 0$ in the box $[x_0, x^\star] \times [0, \beta(x_0)]$, which contains no equilibrium; the solution initiated in $(x_0, \beta(x_0))$ then necessarily exits the box in finite time, hence crosses the $x = x^\star$ line. The upper-bound on T is then

$$T^\star = \inf_{x_0 \in (0, x^\star)} \tau(x_0)$$

that we will have to show to be positive for the control scheme to be applicable. Since $0 < \dot{x} < \max_{[0,x^\star]} f(x)$ for all $x < x^\star$, $\tau(x_0)$ is lower-bounded by $\frac{x^\star - x_0}{\max_{[0,x^\star]} f(x)} > 0$, which only approaches 0 as x_0 goes to $x^\star$. This indicates that the only way that $T^\star$ could be 0 is if $\lim_{x_0 \to x^\star} \tau(x_0) = 0$. For x_0 close to $x^\star$ (and then $(x_0, \beta(x_0))$ close to $(x^\star, y^\star)$) system (2) is equivalent to its linearization

$$\dot{Z} = \mathcal{J} Z$$

with $Z = (\tilde{x}, \tilde{y})^T = (x, y)^T - (x^\star, y^\star)^T$, which has complex conjugate eigenvalues of the form $\lambda = \rho \pm \omega i$:

$$\rho = \frac{1}{2}\left(f'(x^\star) - g'(x^\star)\frac{f(x^\star)}{g(x^\star)}\right) = \frac{1}{2}\mathcal{J}_{11}$$

$$\omega = \sqrt{h'(x^\star)f(x^\star) - \frac{1}{4}\left[\left(\frac{f}{g}\right)'(x^\star)g(x^\star)\right]^2}$$

In the Z space, the solutions rotate around the equilibrium with a period $\frac{2\pi}{\omega}$ and, by symmetry, operate half a revolution in $\frac{\pi}{\omega}$; however, this proportionality is not kept for other angles. The initial condition for the construction of τ_0 (the local approximation of $\tau(x_0)$, which is independent of x_0) is then $(\tilde{x}_0, \tilde{y}_0)^T = (x_0 - x^\star, \beta'(x^\star)(x_0 - x^\star))^T$ and the terminal condition is characterized by $\tilde{x} = 0$. Using Putzer's formula [Putzer, 1966]

$$Z(t) = e^{\rho t}\left[\cos(\omega t) + \frac{\sin(\omega t)}{\omega}(\mathcal{J} - \rho I)\right] Z_0, \qquad (5)$$

$\tau(x_0)$ is then determined by $\tilde{x}(t) = 0$:

$$0 = e^{\rho \tau_0}\left[\cos(\omega\tau_0)\tilde{x}_0 + \frac{\sin(\omega\tau_0)}{\omega}\left((\mathcal{J}_{11} - \rho)\tilde{x}_0 + \mathcal{J}_{12}\tilde{y}_0\right)\right]$$

which indicates that the value of the first coordinate of $Z(t)$ is 0 after time τ_0. This is equivalent to

$$\tau_0 = \frac{1}{\omega}\text{arccotan}\left(-\frac{\rho - g(x^\star)\beta'(x^\star)}{\omega}\right) < \frac{\pi}{\omega} \qquad (6)$$

where we have used $\mathcal{J}_{11} = 2\rho$, $\mathcal{J}_{12} = -g(x^\star)$, and $\tilde{y}_0 = \beta'(x^\star)\tilde{x}_0$. τ_0 clearly is a positive value since the argument of arccotan is not $-\infty$. We then have that $\lim_{x_0 \to x^\star} \tau(x_0) = \tau_0 > 0$ so that the infimum $T^\star$ exists and is positive.

Theorem 1. Let system (4) satisfy Assumptions 1-4, with $T < T^\star$, then equilibrium $(x^\star, y^\star)$ is Globally Asymptotically Stable in the positive orthant.

Proof: We first note that, between impulses, no convergence towards $(x^\star, y^\star)$ can take place because the equilibrium is unstable with complex conjugate eigenvalues.

We will first show that any solution eventually reaches the $y = \beta(x)$ manifold with $x < x^\star$. For that, we will analyze what happens for initial conditions different from the equilibrium for some $t_0 \in (nT^+, (n+1)T]$ in the four regions separated by the $x = x^\star$ and $y = \beta(x)$ manifolds, illustrated on Fig. 1.

Region I ($x \leq x^\star$ and $y < \beta(x)$): Since $\dot{x} > 0$ and $\dot{y} < 0$, the solution cannot go through $y = \beta(x)$ because $\dot{y} - \beta'(x)\dot{x} < 0$; it either enters region II where $x \geq x^\star$ before time $(n+1)T$ or it does not and an impulse takes place that brings the solution to $(x((n+1)T)), \beta(x((n+1)T)))$ with $x \leq x^\star$. In the former case, the solution gets into Region II and can be followed in the next paragraph; in the latter, the target manifold is reached.

Region II ($x > x^\star$ and $y < \beta(x)$): Since $\dot{y} > 0$ and the $x = x^\star$ boundary cannot be crossed because $\dot{x} > 0$ there, the solution either enters region III where $y > \beta(x)$ before time $(n+1)T$ or it does not and an impulse takes place that brings the solution to $(x((n+1)T)), \beta(x((n+1)T)))$ with $x > x^\star$, also in region III.

In the next two regions, no impulse takes place so that they can only be exited through the continuous dynamics.

Region III ($x > x^\star$ and $y \geq \beta(x)$): The solution either:

- has y growing unbounded within the region in finite or infinite time $\tilde{t}$ which, since $x(t)$ is decreasing with $x \geq x^\star$, means that the slope of the solution in the phase plane satisfies $\limsup_{t\to\tilde{t}} \frac{\dot{y}}{\dot{x}} = -\infty$. This cannot be since

$$\frac{\dot{y}}{\dot{x}} = \frac{h(x) - m}{\frac{f(x)}{y} - g(x)}$$

When y grows to large values, this becomes $\frac{h(x)-m}{-g(x)}$ which, for $x \geq x^\star$ cannot go to infinity; this type of solution is not possible.

• exits the region in finite time. We have $\frac{d}{dt}(y - \beta(x)) > 0$ since y is increasing and x decreasing, so that the solution cannot exit through $y - \beta(x)$. The solution then exits the region through $x = x^\star$ towards region IV.

Region IV ($x \leq x^\star$ and $y \geq \beta(x)$): Since $\dot{y} < 0$, the only equilibrium in this region is again $(x^\star, y^\star)$ and since convergence towards the equilibrium cannot take place, the solution necessarily exits the region through $y = \beta(x)$ at some time $t \in [pT, (p+1)T]$, with $p \geq n$. Since $T < T^\star$, an impulse then takes place at time $(p+1)T$ while the solution is in region I; this brings the solution to $(x(p+1)T, \beta(x((p+1)T))$ with $x((p+1)T) < x^\star$.

We have shown that any solution eventually reaches some $(x(nT^+), \beta(x(nT^+)))$ for some n with $x(nT^+) < x^\star$. We will then show where the solution is at time $(n+1)T^+$. During the $(nT^+, (n+1)T]$ time interval, since $y < \frac{f(x)}{g(x)}$ and $x < x^\star$, $\dot{x} > 0$ and $\dot{y} < 0$; the solution then remains in region I where $y < \beta(x)$ and $x < x^\star$; the latter is ensured because $T < T^\star < \tau(x((n)T^+))$, which is the time it takes for the solution to reach $x = x^\star$ and then leave Region I. For any $x(nT^+) < x^\star$, after the impulse at time $(n+1)T^+$, the solution is again on the manifold $y = \beta(x)$, with $x((n+1)T^+) > x(nT^+)$ because $\dot{x} > 0$ in Region I. The sequence $(x(nT^+))_{n\in\mathbb{N}}$ then eventually goes to $x^\star$.

We have shown global attractivity of the equilibrium. Its asymptotic stability is similar in spirit. For an initial condition close to the equilibrium, the time it takes for the solution to reach the manifold $y = \beta(x)$ with $x < x^\star$ is smaller than $2T + \frac{\pi}{\omega}$ (the summation of three terms: 1) T, the maximum time it takes for a solution to reach $y \geq \beta(x), x > x^\star$; 2) $\frac{\pi}{\omega}$, the time it takes for a solution to locally go from $y = \beta(x)$ with $x > x^\star$ to $y = \beta(x)$ with $x < x^\star$ through half a revolution; 3) T, the maximum time it takes before the first impulse after $y = \beta(x)$ with $x < x^\star$ has been reached. During that finite time, the solution slowly drifts away from the equilibrium; however, if for stability we wish to keep $(x(t), y(t))$ in an ϵ-neighborhood of the equilibrium, it suffices to take the initial condition sufficiently close to the equilibrium; after the drifting part, convergence takes place along $y = \beta(x)$ so that the solution still stays in the ϵ-neighborhood, hence stability is shown. □

The way these solutions converge towards the equilibrium is illustrated on Fig. 3.

4. BEYOND THEOREM 1

4.1 Larger T values

In order to obtain global stability for T larger than $T^\star$, one would need to consider the Poincaré map [Guckenheimer and Holmes, 1983] with solutions possibly rotating around the equilibrium. With the generality of the functions that we presented, it is however not easy to handle. Therefore, in order to consider larger T values, we concentrate on local attractivity once the solution has reached the manifold $y = \beta(x)$ or, locally, $\tilde{y} = \beta'(x^\star)\tilde{x}$ with $\tilde{x}, \tilde{y} < 0$. Two cases can easily be handled.

Multiple oscillations: $\frac{(2k-1)\pi}{\omega} + T^\star < T < \frac{2k\pi}{\omega} + T^\star$ Let us first consider T satisfying $\frac{2k\pi}{\omega} < T < \frac{2k\pi}{\omega} + T^\star$, with $T^\star$ given by the local approximation obtained in (6) and the initial condition $(\tilde{x}, \tilde{y})^T = -\epsilon\,(1, \beta'(x^\star))^T$ with $\epsilon > 0$ small. As previously said, the solution hits back on the $\tilde{y} = \beta'(x^\star)\tilde{x}$ manifold every $\frac{\pi}{\omega}$ time-instants, so that it is back on the manifold, with $\tilde{x}, \tilde{y} < 0$ at time $\frac{2k\pi}{\omega}$. Since $0 < T - \frac{2k\pi}{\omega} < T^\star$, the solution does not stop at the manifold but does not go beyond $\tilde{x} = 0$ (or $x = x^\star$) either. The impulse brings the solution back on the manifold. We then just have to check if it is on the right of the initial condition. Through Putzer's formula (5),

$$\tilde{x}(T) = e^{\rho T}\left[\cos(\omega T)(-\epsilon) + \frac{\sin(\omega T)}{\omega}(-\rho\epsilon + g(x^\star)\beta'(x^\star)\epsilon)\right] \tag{7}$$

and convergence takes place if $0 > \tilde{x}(T) > -\epsilon$, that is if

$$0 < e^{\rho T}\left[\cos(\omega T) + \frac{\sin(\omega T)}{\omega}(\rho - g(x^\star)\beta'(x^\star))\right] < 1 \tag{8}$$

Defining $\tilde{T} = \mathrm{mod}(T, 2\pi)$ and $2k\pi = T - \tilde{T}$, this is equivalent to

$$e^{\rho\tilde{T}}\left[\cos(\omega\tilde{T}) + \frac{\sin(\omega\tilde{T})}{\omega}(\rho - g(x^\star)\beta'(x^\star))\right] < e^{-2k\pi\rho}$$

For $\tilde{T} = T^\star$, the inequality is strictly satisfied because the left-hand side is zero. The bigger k, the smaller the $\tilde{T}$-interval $(\tilde{T}_k, T^\star]$ in which it is satisfied because the upper-bound $e^{-2k\pi\rho}$ decreases. For these values of $\tilde{T}$, we have local asymptotic stability of the equilibrium.

Note that a similar reasoning can be held for $\frac{(2k-1)\pi}{\omega} + T^\star < T < \frac{2k\pi}{\omega}$. The reference initial conditions are then on $\epsilon\,(1, \beta'(x^\star))^T$ with $\epsilon > 0$. The chosen periods then ensure that, locally, a solution initiated on that part of the manifold, ends up in Region I after a period T, so that an impulse ensues that brings the solution back on $\tilde{y} = \beta'(x^\star)\tilde{x}$. A stability analysis on that manifold also yields condition (8).

Short periods: $T^\star < T < \frac{\pi}{\omega}$ With such a choice of T, a solution can potentially go through Region I without impulse. We can then consider two reference situations: the study of the evolution of the impact points on the $\tilde{y} = \beta'(x^\star)\tilde{x}$ manifold for $\tilde{x} > 0$ or $\tilde{x} < 0$ initially.

In the $\tilde{x} > 0$ case, we consider an initial condition $(\tilde{x}, \tilde{y}) = \epsilon\,(1, \beta'(x^\star))^T$ for which the system's dynamics drive the system into regions III and IV where $\tilde{y} > \beta'(x^\star)\tilde{x}$ and where no actual impulse occurs. Since $T < \frac{\pi}{\omega}$ one or several measurement instants take place with the state in that region. In order to quickly conclude, we suppose that no impulse takes place in region I and that the first impulse then takes place after the system has reached Region II.

With the last measurement instant in the regions (III and IV) where $\tilde{y} > \beta'(x^\star)\tilde{x}$ being $T_\sharp = \frac{\pi}{\omega} - \text{mod}\left(\frac{\pi}{\omega}, T\right)$, that is the largest multiple of T smaller than $\frac{\pi}{\omega}$, this means that the impulse takes place at time $T_\sharp + T$ with

$$T_\sharp + T = \frac{\pi}{\omega} - \text{mod}\left(\frac{\pi}{\omega}, T\right) + T > \frac{\pi}{\omega} + T^\star$$

or

$$T^\star < T - \text{mod}\left(\frac{\pi}{\omega}, T\right) < T < \frac{\pi}{\omega} \tag{9}$$

The condition for convergence is then that, $\tilde{x}(T_\sharp + T) < \epsilon$, which directly translates into

$$0 < e^{\rho(T_\sharp+T)}\left[\cos(\omega(T_\sharp + T)) + \frac{\sin(\omega(T_\sharp + T))}{\omega}\left(\rho - g(x^\star)\beta'(x^\star)\right)\right] < 1 \tag{10}$$

which, coupled with (9), ensures local stability.

In the $\tilde{x} < 0$ case, the image of $-\epsilon\left(1\ \beta'(x^\star)\right)^T$ is studied. A first impulse then takes place in region II after time T, and the second impulse occurs once the solution is back in region I. After computations similar to those above, we see that stability then hinges on conditions

$$T - \text{mod}\left(\frac{\pi}{\omega}, T\right) < T^\star < T < \frac{\pi}{\omega} \tag{11}$$

which is complementary to condition (9) and

$$0 < e^{\rho(2T+T_\sharp)}\left[\cos(\omega T) + \frac{\sin(\omega T)}{\omega}\left(\rho - g(x^\star)\beta'(x^\star)\right)\right]\left[\cos\left(\omega(T + T_\sharp)\right) + \frac{\sin\left(\omega(T + T_\sharp)\right)}{\omega}\left(\rho - g(x^\star)\beta'(x^\star)\right)\right] < 1 \tag{12}$$

4.2 Controllability of the equilibrium

If Assumption 3 is not satisfied, most of the proof of Theorem 1 stays valid. There is no obstacle to global attractivity. However, the last part that shows stability cannot be achieved: the eigenvalues are both positive real (since $\det(\mathcal{J}) > 0$), so that a solution in region IV close to the equilibrium will be steered away from the equilibrium by the eigenvectors, instead of rotating towards region I. Eventually, the solution will leave region IV towards region I, but it might be far from $(x^\star, y^\star)$ by then. As with the controller of Grognard et al. [2013], $(x^\star, y^\star)$ is globally attractive and unstable.

5. ILLUSTRATION

All these theoretical developments need to be illustrated on a simple model. We opted for the Rosenzweig-MacArthur model (1) with the parameters $r = 1$, $K = 1$, $b = 1$, $c = 2$, $m = 1.5$ and $h = 0.1$. We chose one of the simplest functions $y = \beta(x)$, that is the linear function $y = 0.8x + 0.04$, which goes through the unstable equilibrium $(x^\star, y^\star) = (0.3, 0.28)$. Preliminary computations yield $\rho = 0.1125$ and $\omega = 0.4998$.

5.1 Global stability

On Fig. 2, we illustrate function τ as a function of $x < x^\star$, as expected, when x gets close to 0, $\tau(x)$ goes to infinity because $\dot{x}$ becomes very small and, when x approaches $x^\star$, $\tau(x)$ becomes close to what was predicted by formula (6), that is $\tau_0 = 1.596$. In the present study, $T^\star$ is given by these initial conditions close to $x = x^\star$ but this is not always the case.

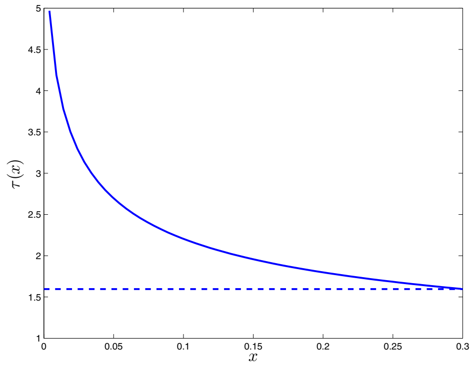

Fig. 2. Illustration of function $\tau(x)$ which indicates the time it takes for a solution to go from the line $y = 0.8x + 0.04$ to the vertical line $x = 0.3$ as a function of the abscisse x of the initial condition (solid line).

For $T < T^\star = 1.596$, Theorem 1 indicates that the positive equilibrium is globally asymptotically stable in the positive orthant. This is illustrated for $T = 1.1$ on Fig. 3, in the (x, y) space, where it can be seen that a first impulse takes place after a time T and then that at the end of the next 4 periods no jump takes place. The system reaches the region where it slides along the $y = \beta(x)$ manifold through repeated jumps and converges towards the equilibrium. From Fig. 3, we can infer that if T tends to 0, this controller will become similar to a sliding-mode controller along $\beta(x)$.

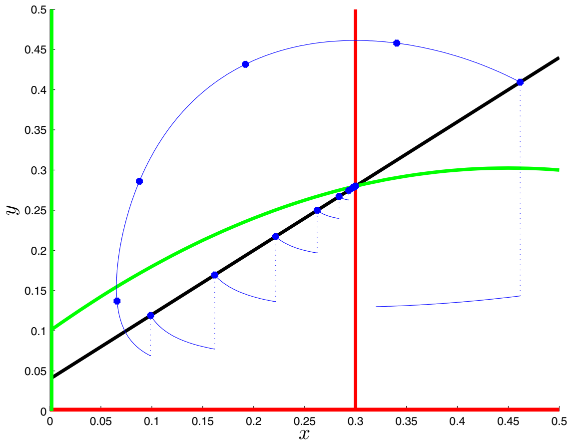

Fig. 3. Illustration of the evolution of a solution with $T = 1.1$ and initial condition $(0.32, 0.13)$ in the (x, y) state-space. The solution is in blue; the measurement instants are indicated by blue stars.

5.2 Larger T values

The numerical construction of the expression in inequality (8) and the analysis of the T-intervals where it is in $[0, 1]$ yields local asymptotic stability in the intervals $(0, 1.596)$ (as previously), $(7.881, 8.442)$, $(13.864, 14.167)$, $(20.452, 20.593)$,... As explained in the theoretical part, these intervals become smaller and smaller with larger T.

The numerical analysis of conditions (9)-(10) and (11)-(12) yields additional regions where the equilibrium is locally asymptotically stable: the intervals $(1.596, 2.814)$ and $(3.778, 4.221)$. We see that the safe region with T small is much larger the obtained through Theorem 1: one can pick $T \in (0, 2.8143)$ and ensure stability. The other stability intervals are more restricted and, since parameters are little known, there is a big risk of instability if one chooses such a T.

5.3 Asymptotic analysis

We now numerically study the asymptotic behavior of the closed-loop system as a function of T by analyzing Fig. 4. This figure illustrates, for the initial condition $(0.31, 0.288)$, what the impact points following impulses are on the manifold $y = \beta(x)$; we only consider the asymptotic behavior so that we only illustrate the x coordinate of the impulses after the solution has settled on some attractor. As expected, we recover asymptotic stability in the T-intervals that we have identified previously; these are recognized by the fact that $x^\star = 0.3$ is the lone asymptotic point. However, some other regions come up: in the interval $(6.95, 7.20)$, which we had not found theoretically, the equilibrium is also attractive. Note that other illustrated asymptotic behaviors correspond to cases where 1, 2 and 4 different impulses take place in the asymptotic solution; the latter occurs for T close to 4.6. Above $T = 29.65$ (pseudo?)-chaotic behavior occurs. The construction of a bifurcation diagram including all possible asymptotic behaviors, such as the nested unstable and stable limit cycles for $2.673 < T < 2.814$, is the object of future work.

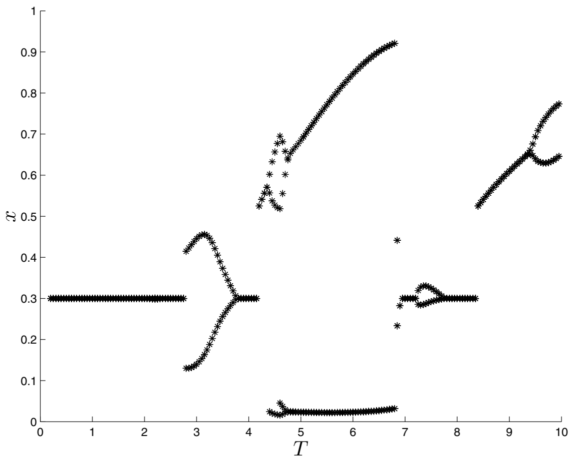

Fig. 4. Asymptotic value of x as a function of T for the initial condition $(0.31, 0.288)$. When the asymptotic value is $x = 0.3$, the equilibrium is reached. Otherwise, the x coordinate of impact points on the $y = \beta(x)$ manifold are illustrated.

6. CONCLUSION

We have proposed a control method that merges the advantages of two pre-existing control methods for biological control: it corresponds to the way biocontrol agents are released since it is impulsive and it has the robustness of a feedback controller. That way, we have been able to show global asymptotic stability of the desired equilibrium provided the monitoring period is small enough. Beyond that, complex behaviors have been evidenced through numerical and asymptotic analyses: for large T-values, the impulses excite the system's dynamics. Further developments should be carried out in order to better understand the bifurcation diagram, to introduce the effect of noise, the inaccuracy in the equilibrium determination due to model uncertainties, study transient and the bioeconomic aspects. Though the model is a simplification of the dynamics that actually take place in biological control systems, we believe that it gives ideas on how to develop new biological control strategies.

REFERENCES

R.F. Brammer. Controllability in linear autonomous systems with positive controllers. *SIAM Journal on Control*, 10:339, 1972.

R.T. Bupp, D.S. Bernstein, V.S. Chellaboina, and W.M. Haddad. Resetting virtual absorbers for vibration control. *Journal of Vibration and Control*, 6:61–83, 2000.

F. Grognard and J.-L. Gouzé. Positive control of Lotka-Volterra systems. In *Proceedings of 16th IFAC World Congress, Prague, Czech Republic*, 2005.

F. Grognard, J. Rault, and J.-L. Gouzé. Positive control for global stabilization of predator-prey systems. In *Proceedings of 9th IFAC Symposium Nonlinear Control Systems (NOLCOS'13), Toulouse, France*, 2013.

J. Guckenheimer and P. Holmes. *Nonlinear Oscillations, Dynamical Systems, and Bifurcations of Vector Fields.* Springer-Verlag, New York, 1983.

W.M. Haddad, V.S. Chellaboina, and N.A. Kablar. Active control of combustion instabilities via hybrid resetting controllers. In *Proceedings of the American Control Conference*, volume 4, pages 2378–2382, 2000.

W.M. Haddad, V.S. Chellaboina, and S.G. Nersesov. *Impulsive and Hybrid Dynamical Systems.* Princeton University Press, 2006.

B.A. Hawkins and H.V. Cornell. *Theoretical Approaches to Biological Control.* Cambridge University Press, 1999.

B. Liu, Y. Zhang, and L. Chen. Dynamic complexities of a Holling I predator-prey model concerning periodic biological and chemical control. *Chaos, Solitons & Fractals*, 22(1):123 – 134, 2004.

L. Mailleret and F. Grognard. Global stability and optimisation of a general impulsive biological control model. *Mathematical Biosciences*, 221(2):91 – 100, 2009.

M.E.M. Meza, A. Bhaya, E. Kaszkurewicz, and M.I. da Silveira Costa. Threshold policies control for predator-prey systems using a control Liapunov function approach. *Theoretical population biology*, 67(4):273–284, 2005.

E.J. Putzer. Avoiding the Jordan canonical form in the discussion of linear systems with constant coefficients. *The American Mathematical Monthly*, 73:2–7, 1966.

M.L. Rosenzweig. Paradox of enrichment: destabilization of exploitation ecosystems in ecological time. *Science*, 171(3969):385, 1971.

S.H. Saperstone and J.A. Yorke. Controllability of linear oscillatory systems using positive controls. *SIAM Journal on Control*, 9:253–262, 1971.

V. Volterra. Variations and fluctuations in the number of coexisting animal species (1927). In F.M. Scudo and J.R. Ziegler, editors, *The golden age of theoretical ecology: 1923-1940*, pages 65–234. Springer-Verlag, 1978.